ELSEVIER

Ceramics International 25 (1999) 593–599

CERAMICS INTERNATIONAL

The effect of ZnO on the sintering and stabilization of ZrO_2.MgO system

R.S. Nasar [a,*], M. Cerqueira [a], E. Longo [b], J.A. Varela [c]

[a] *Departamento de Química, UFRN, Natal, RN, 59072-970, Brazil*
[b] *Departamento de Química, UFSCar, São Carlos, SP, 13565-905, Brazil*
[c] *Instituto de Química, UNESP/Araraquara, SP, 14800-900, Brazil*

Received 30 June 1998; received in revised form 17 July 1998; accepted 2 September 1998

Abstract

The sintering of ZrO_2.MgO.ZnO powder has been investigated by TMA (Thermal Mechanical Analyser) and its phases analysed by XRD (X-ray diffraction pattern). The data obtained from sintering was studied by the Bannister equation and its dominant sintering mechanism was calculated. It was observed that the ZnO addition in the ZrO_2.MgO solid solution lead to increased zirconia stabilization. According to the vacancies model, the ZnO addition did not lead to zirconia phases stabilization (PSZ). An analysis of the rate control in the initial stage of the sintering (region I) showed a mechanism of volume diffusion type. In other regions (regions II and III), the grain growth did lead to the Bannister equation deviation, which was observed by SEM (Scanning Electron Microscopy). These results were different from those demonstrated by other authors who studied the $ZrO_2.Y_2O_3$ solid solution and obtained a mechanism of grain boundary diffusion type.

Keywords: Magnesia–PSZ; Bannister equation; Zirconia stabilization

1. Introduction

Several investigators [1,2] have successfully used the theory proposed by Frenkel [3] in describing the viscous sintering of glass. This model, which was applied to the isothermal techniques, was modified by the introduction of the constant rate of heating ($a = dT/dt$) term which are more consistent with industrial sintering conditions. The technique was used for data describing thermoluminescence [4] correlated with exponential relations describing first-order reactions. Other authors [5,6] studied thermoconductivity and chemical reactions, both with the use of the constant rate of heating (CRH) method.

Cutler [7], who studied spherical glass compacts observed that good agreement exists on the determination of temperature dependence on sintering and shrinkage with the use of CRH technique. As a Frenkel equation modification, Johnson [8] proposed a model with only one equation by simultaneous determination of the volume and grain-boundary diffusion of spherical crystalline particles. However, one more mechanism could occur at the same activation energies was observed by using a slower rate control process. Young and Cutler [9] treated the variables of the Johnson equation on observation that the grain boundary and the mechanism of volume diffusion type occurred separatelly. The data analysis of the partially stabilized zirconia (PSZ) samples, by these equations, showed that if the volume diffusion kinetics predominate, the activation energy, Q, is 60 Kcal/mol. Grain boundary diffusion kinetics gave 90 Kcal/mol, improving those values that were reported by Jorgensen [10].

According to the Bannister study [11], the equation of an initial-stage sintering rate in the CRH method was as follows:

$$d\left(\frac{\Delta L}{Lo}\right)/dt = k/\left(\frac{\Delta L}{Lo}\right)^n \quad (1)$$

where $\frac{\Delta L}{Lo}$ is the linear shrinkage, Lo and L are the initial and final samples length, t is time, n is a constant related to the dominant mechanism of sintering.

For a sintering based on a viscous flow mechanism, it depends on Frenkel's equation and is expressed by: k, that is roughly expressed as follows with respect to temperature,

* Corresponding author. Tel.: +55-084-2153823; fax: +55-084-2119224.
E-mail address: nasar@linus.quimica.ufrn.br (R.S. Nasar)

0272-8842/99/$ - see front matter
PII: S0272-8842(98)00070-4

$k = ko\exp(-Ea/RT)\ dt$ is the rate constant and (2)

$$k = (3\gamma/8r\eta) \qquad \text{and } n = 0 \tag{3}$$

In the case of sintering of spherical particles, Woolfrey [12] proposed the following equations: Sintering by volume diffusion:

$$k = (1.95\gamma\Omega Dv/\kappa r^3 T) \qquad \text{and } n = 1 \tag{4}$$

Sintering by boundary diffusion:

$$k = (0.48\gamma\Omega Db/\kappa r^4 T) \qquad \text{and } n = 2.1 \tag{5}$$

where:

$\eta =$	viscosity
$\gamma =$	surface energy
$\Omega =$	the volume of a transported compound per an ion or an atom of the diffusing species
$Dv, b =$	diffusion coeficients
$\delta =$	neck width
$\kappa =$	Boltzmann's constant
$r =$	particle diameter
$T =$	absolute temperature

Substituting Eq. (2) and a constant-rate heating condition $a = dT/dt$ into Eq. (1) the following is obtained:

$$(\Delta L/Lo)^n = [(n+1)/\mathrm{a}] \int_{To}^{T} ko\exp(-Ea/RT)dT, \tag{6}$$

$Ea =$ Activation Energy
$R =$ Gases Constant

Ordinarily, shrinkage at low temperatures can be negleted and the equation is adjusted as follows:

$$\int_{To}^{T} \exp(-Ea/RT)dT = \int_{o}^{T} ko\exp(-Ea/RT)dT \tag{7}$$

when Ea is greater than RT, Eq. (6) can rougly be rewritten as follow:

$$\left(\frac{\Delta L}{Lo}\right)^{n+1} = [koRT^2(n+1)/aEa] \int_{0}^{T} \exp(-Ea/RT) \tag{8}$$

the term:

$$\frac{koRT(n+1)}{Ea} = C \tag{9}$$

substituting Eq. (9) into (8) obtains,

$$\left(\frac{\Delta L}{Lo}\right)^{n+1} = a^{-1}C\exp(Ea/RT) \tag{10}$$

the term:

$$C\exp(-Ea/RT) = C^* \tag{11}$$

substituting C^* into Eq. (10) obtains,

$$(\Delta L/Lo)^{n+1} = -aC^* \tag{12}$$

Applying the Log function for both terms,

$$\ln(\Delta L/Lo) = -(1/(n+1))\ln a + \ln C/(n+1) \tag{13}$$

A plot $\ln\Delta L/Lo$ versus $\ln a$ obtains the dominant mechanism sintering with slope equal $-(1/(n+1))$.

2. Experimental procedures

2.1. Powder processing

High purity materials (Table 1) was used for the processing of ZrO_2.MgO.ZnO solid solution by conventional route. The basic composition was ZrO_2/MgO with (88.71%/11.29%) molar ratio and the addition of 0.5 mol % of ZnO. The area of the powder precursors surfaces were measured by BET method with an ASAP 2000 of the Micromeritics and the particles size by an Micromeritics sedigraph.

Raw materials were grinded for 6 h with ethyl alcohol and zirconia pellets. The resultant mixture of powders were dried and sieved on 325 meshes. Samples of cylindrical shape with 6 mm of diameter were prepared by uniaxial, 10 MPa and Isostatic, 150 MPa pressed. Green density of the samples were measured and submitted to the Thermo-Mechanical Analyser.

2.2. Constant rate of heating

The CRH method was used with rates of 5, 10, 15 and 20°C/min. The temperature was as high as 1600°C, and started at 100°C for all samples. At 1600°C the furnace was cooled until the ambient temperature and the density of the samples were measured. The Thermo-Mechanical Analyser used was a Netzsch dilatometer model 402 E.

Table 1
Raw materials, particle size (μm) and surface area (m^2/g)

Reagents	P.S. (μm)	S.A. (m^2/g)
ZrO_2	1.80	5.20
MgO	1.10	2.80
ZnO	0.70	5.60

2.3. Rietveld method

This method consists of a comparison between a calculated X-ray diffraction pattern starting to defined crystallographic parameters and an experimental spectrum. Experimental peaks were obtained by a scanning process step by step with constant increment and time, at the multiphase analysis, following:

$$\mathrm{Yec} = \sum_h J_h L P_h F^2 G(\Delta\theta_{ih}) P_h + Yb_i$$

$S=$	Scale factor,
$J_h=$	Multipicity,
$L=$	Lorentz factor,
$P_h=$	Polarization factor,
$F=$	Structure factor,
$\Delta\theta=$	ith θ angle,
$Yb_i=$	Next peak contributions

An approximation between the observed X-ray diffraction and the calculations were made by minimum squares with the use of a lorentzian curve type.

New refined parameters were obtained from the X-ray diffraction profile calculated. Both the refined profile and the phases deconvolution were obtained from the peaks of the X-ray diffractogram.

2.4. SEM observations

Scanning electron microscopy (SEM) was used for the microstructural analysis. The surface of the samples was polished with alumina (0.1–1.0 μm) and diamond (0.3, 0.1 μm), and then, etched by chemical solution of HCl/HNO_3-(1/1), with acid (1/5 vol%) and alcohol (4/5 vol%). Gold was deposited by sputtering on the samples and their surfaces were observed. A SEM JEOL model JSM-T 330A was used.

3. Results

3.1. Phases formation and linear shrinkage

The X-ray diffraction patterns of the ZrO_2.MgO solid solution sintered until 1600°C with a heating rate of 10°C/min. showed the partial stabilization of zirconia (PSZ) [13], (Fig. 1). It was observed that the addition of 0.5 mol % of ZnO lead to increases of tetragonal (t) and cubic (c) phases. The increases of stabilized phases, calculated by the Rietveld method [14], was from 51.23% c and 18.32% t to 9.62% c and 84.13% t, respectively.

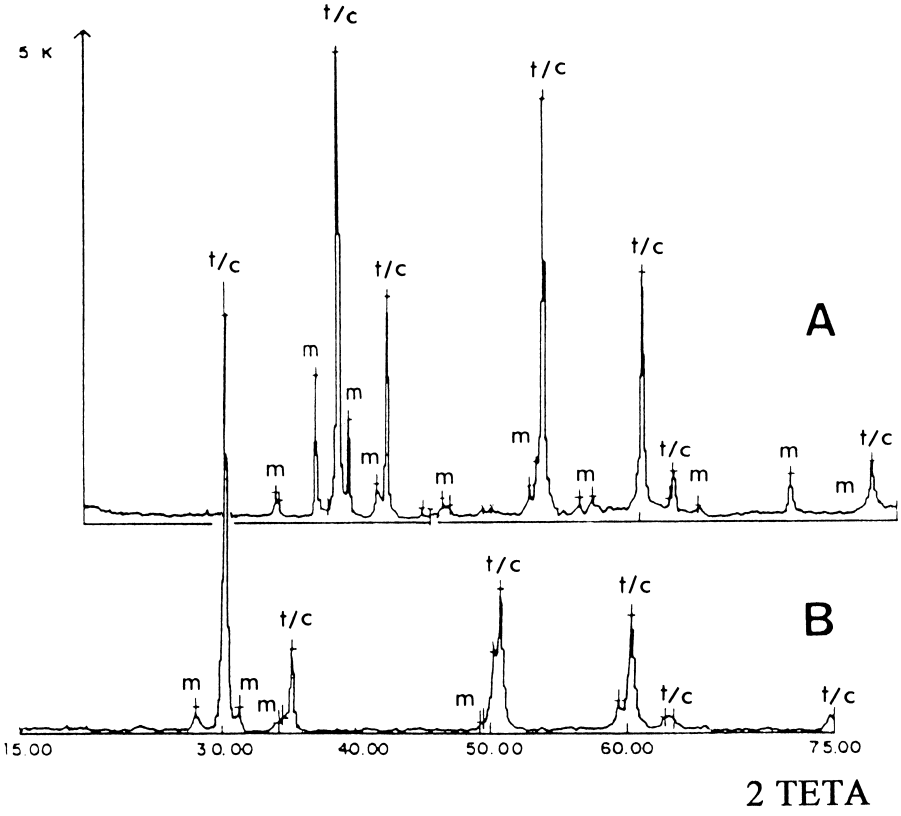

Fig. 1. X-ray diffraction patterns of the zirconia phases sintered until 1600°C, 10°C/min. A: ZrO_2.MgO phases with (88.71%/11.29%) molar ratio; B: ZrO_2.MgO.ZnO phases with (88.71%/10.79%) and 0.5 % of ZnO.

These results didn't agree with the model that considered the zirconia stabilization caused only by ions formers of substitutional solid solution [15].

Fig. 2 shows the Arrhenius plotting of the shrinkage behaviour of ZrO_2.MgO.ZnO phases. It was observed, by using heating rates (5–20°C/min), two inflection points by each rate. This inflection points indicated that the sintering proceeded in three stages. At the intermediary stage (II) points are coincident for all rates and at the final stage (III) parallel points occurred for different rates. However, due to the grain growth, the Bannister equation was used at the initial stage of sintering, stage (I).

Fig. 3 shows a rapid increase of apparent density above of 1050°C with a heating rate of 20°C/min. At the first sintering stage, from 900–1050°C, which is below the monoclinic/tetragonal phases transition of zirconia, an increased 10% with values about 3.7 g/cm^3 were observed and at 1600°C values about 5.7 g/cm^3 were obtained.

3.2. Sintering mechanism and grain size

Analysis by SEM, at 1000 and 1100°C, [Fig. 4(a) and (b)] shows small grains with an incomplete formation and with a high residual porosity. [Fig. 4(c) and (d)], at 1400 and 1600°C, respectively shows that a strong grain growth occurs.

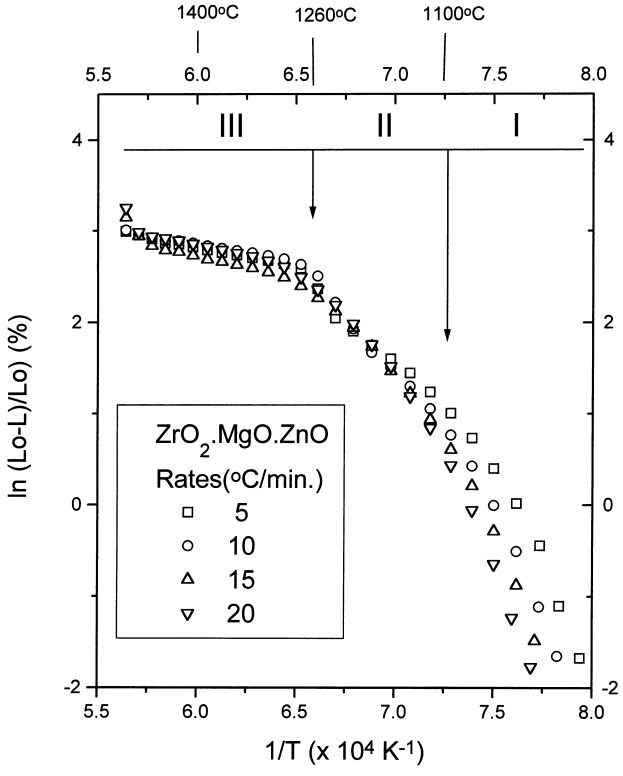

Fig. 2. Arrhenius plotting, $\ln[(L - Lo)/Lo]$ versus $1/T$ of shrinkage behavior of the ZrO_2.MgO.ZnO phases. Rates of 5, 10, 15 and 20°C/min.

Fig. 5 shows a rapid grain growth from 900 to 1000°C, and after this a small increase of grain sizes from 1000 to 1100°C were observed, both regions in the stage I of sintering.

At the stages I and II, a rapid grain growth occurred reaching nearly 5.0 μm at 1600°C. Therefore, the grain growth, after the stage I, occurred with the increase apparent density, (Fig. 3).

Fig. 6 shows the results obtained by the sintering mechanism of the initial stage (I) with the use of the Bannister equation, [Eq. (13)]. It was observed that, up to 1000°C, the n values were incoherent. From 1005 to 1040°C the values were about 1.12 and after 1090°C were above to 3.5. The results (about 1.12), according to the Bannister equation [16], are characterized by an mechanism of volume diffusion type.

These results don't agree with those obtained by Young and Cutler who reported about the zirconia sintering mechanisms. The dominant mechanism accepted was of the grain boundary diffusion type. It was observed that the initial stage was not dominated by the superficial diffusion mechanism type. This mechanism is generally dominant and leads to the neck growth between particles during the initial stage of sintering by a solid state reaction.

4. Discussion

It is observed that the initial stage of the sintering is characterized by the neck formation between particles and generally, after this, a microstructural rearrangement occurs. The mechanism of superficial diffusion type is frequently associated with a mechanism of low activation energy and it is dominant at the initial stage of the sintering, however, the data analysis, Fig. 6 showed a mechanism of volume diffusion type. Other authors [17,18], who studied the $ZrO_2.Y_2O_3$ solid solution obtained a mechanism of grain boundary diffusion type, which lead to the ceramics body shrinkage. It isn't disregarded that, down to the shrinkage temperature, it is possible a superficial diffusion mechanism type occurs, and so, after the initial linear shrinkage it would show other dominant diffusion mechanisms. The CRH method isn't indicated when various mechanisms are present because the Bannister equation is limited to only one mechanism and doesn't accept an overlap between two or more diffusion processes. In the case of mechanism overlaps with different activation energies it was observed only the mechanism with a slower rate control process.

The zirconia stabilization, with the addition of Y, Ce, Mg, Ca and others, occurs with the defects formation due the lattice electroneutrality, and so, in the present case, two processes are concurrent in the solid state diffusion, first; a solid solution formation, second a shrinkage with densification. Both processses occur due

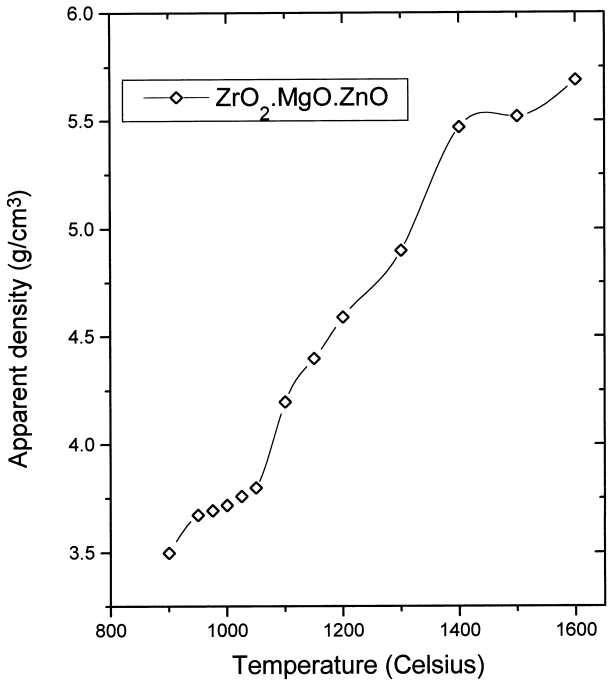

Fig. 3. Apparent density versus sintering temperature of the ZrO_2.MgO.ZnO samples.

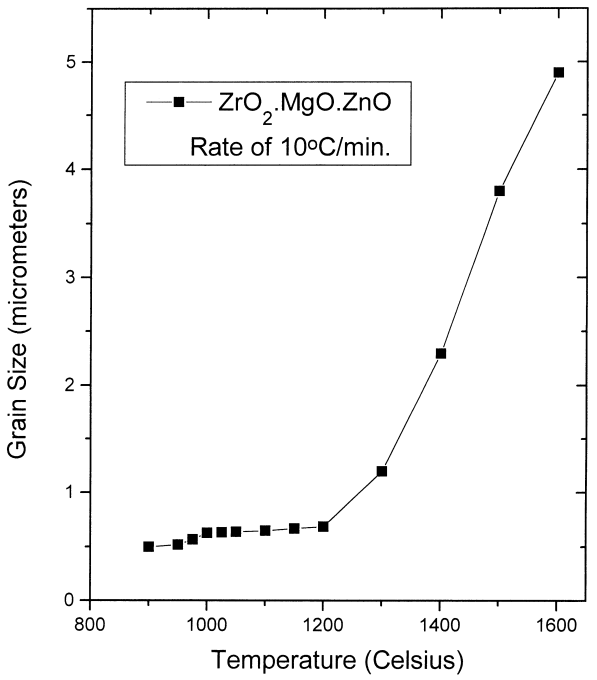

Fig. 5. Grain growth versus sintering temperature of the ZrO_2.MgO.ZnO samples.

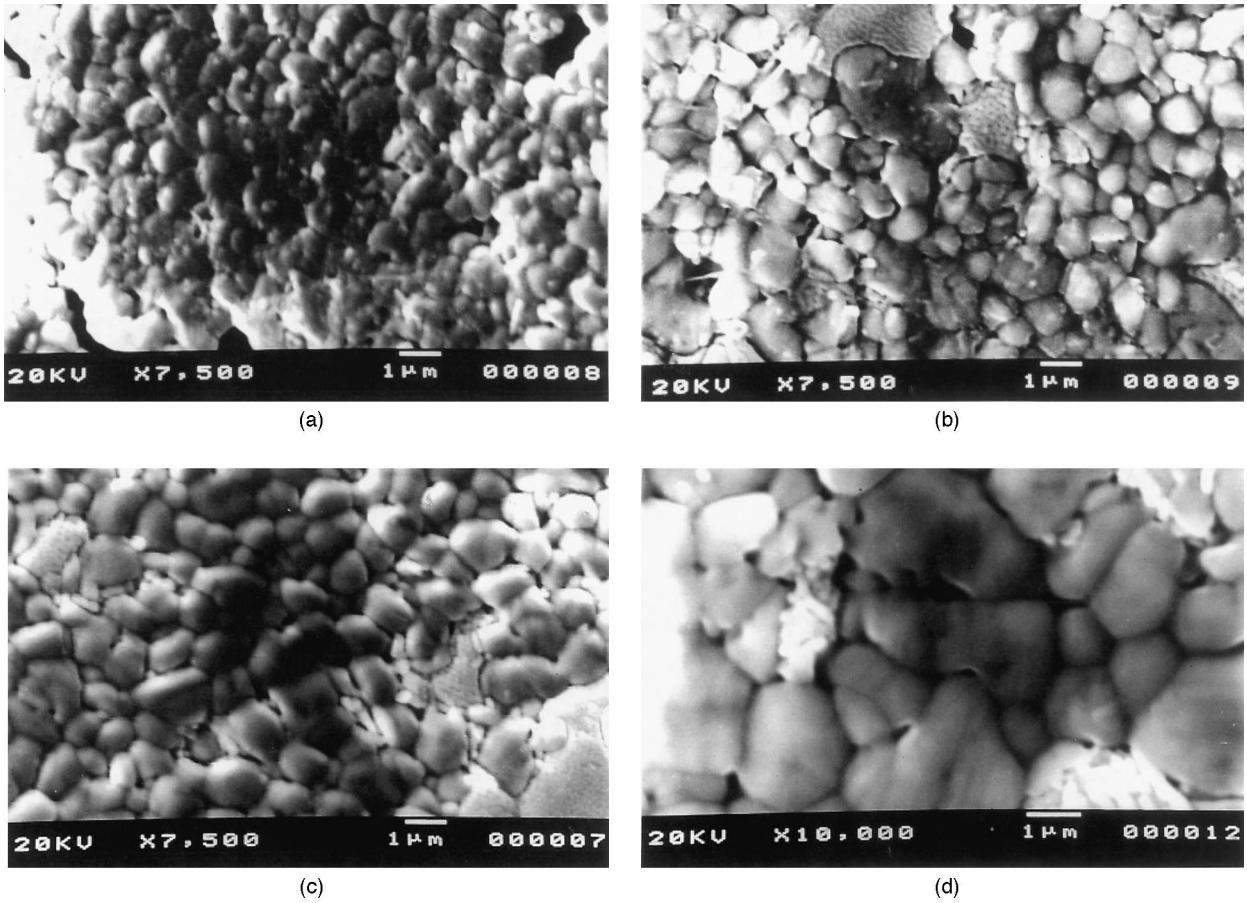

Fig. 4. Scanning electron microscopy of the system ZrO_2.MgO.ZnO. (a): 1000°C; (b): 1100°C; (c): 1400°C; (d): 1600°C. Rates of 10°C/min.

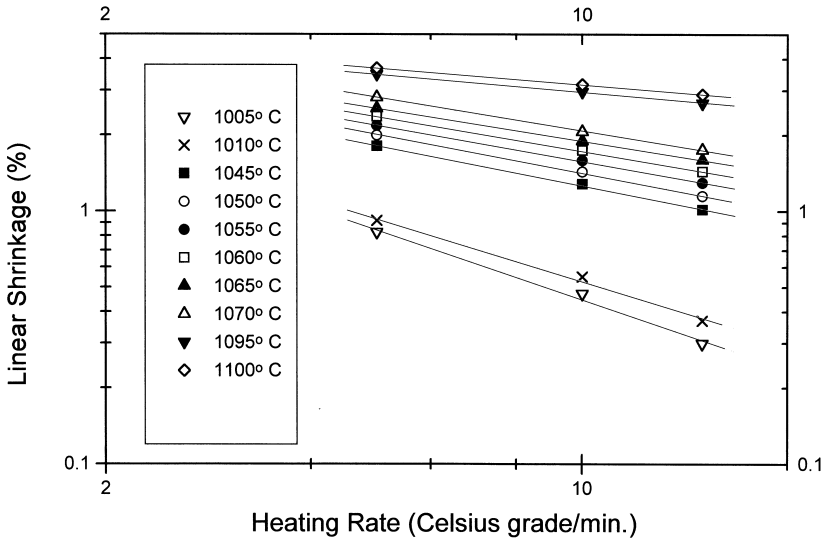

Fig. 6. Logarithm of linear shrinkage versus logarithm of heating rate. The rate control of sintering mechanism.

to a strong chemical potential gradients with high defects concentration (VÖ), when it is thermally activated. The solid state reaction, with the ZrO_2.MgO (Mg^{2+}) solid solution, occurs with the formation of two vacancies, by volume unity, relative to the $ZrO_2.Y_2O_3$ (Y^{3+}) phases, in this way, elements with different valencies would lead to alter the kinetics of the sintering process. At the case of Zn^{2+} addition in the zirconia matrix, despite causing an observed increase in the stabilized phases, it didn't lead to the solid solution formation according to the Dietzel and Tober rules [19] and which is partially accepted by the Hume-Rothery rules [15] and by the model of researches of the National Bureau of Standards (NBS) [20]. The stabilization effects, for some authors [21,22] is attributed to the vacancies formation into the lattice, however, a solid solution between ZrO_2 and ZnO with the vacancies formation was not totally accepted [23]. Then, the effect of ZnO doping may be explained by an increased kinetic effect of the PSZ formation.

Analysis such as the powder morphology and the grain growth at the initial stage of the sintering, (region I) shows particle sizes from 0.6 to 3.1 μm and due to this it didn't contribute to the grain growth, which was caused by the presence of small particles near to the neck between large particles. In a general analysis of the region I, it was observed that, the linear shrinkage started near to 950°C, (Fig. 2) and showed an approximately constant apparent density from 950 to 1050°C, (Fig. 3) and in the same region, the grain growth from 1000 to 1100°C was very small, Fig. 5. The microstructure analysis, [Fig. 4(a) and (b)] between these temperatures showed that, a small alteration of the grain size occurred.

These results show that the calculated sintering mechanism from 1000 to 1100°C doesn't have influenced due to the powder morphology and of the grain growth. Above 1150°C, both the density and the grain growth occurs exponentially with a grain growth from 2 μm at 1400 to 5 μm at 1600°C, Fig. 4(c) and (d). The Bannister equation, which is based on the theoretical sintering of the diffusion model formulated by Frenkel, is only accepted for spherical particles and where the grain growth doesn't alter the densification kinetics and these alterations would lead to the Bannister equation deviations.

The data analysis above show that, at the regions II and III (above 1100°C), the grain growth leads to the Bannister equation deviation, and so, the study of these regions demonstrated incoherent results.

Acknowledgements

The authors acknowledge CNPq and FAPESP for the financial support of this work.

References

[1] W.D. Kingery, J. Appl. Phys. 26(10) (1955) 1205.
[2] G.C. Kuczynsky, I. Zaplatynskyj, J. Am. Ceram. Soc. 39(10) (1956) 349.
[3] J. Frenkel, J. Phys. (USSR), 9(5) (1945) 385.
[4] G.F.J. Garlick (Ed.), Handbuck der Physik, S. Flugge, Springer-Verlag, Berlin, 1958.
[5] G. Bucci, R. Fieschi, Phys. Rev. Letters 12(1) (1964) 16.
[6] T.R. Ingraham, Proc. 1st Toronto Symp. Thermal Anal., Toronto, 1965, 81 pp.
[7] I.B. Cutler, J. Am. Ceram. Soc. 52(1) (1969) 14.
[8] D.L. Johnson, J. Appl. Phys. 40(1) (1969) 192.
[9] W.S. Young, I.B. Cutler, J. Am. Ceram. Soc. 53(12) (1970) 659.
[10] D.L. Johnson, L. Berrin, in: G.C. Kuczinsky, N.A. Hooton, C.F. Gibbon (Eds.), Sintering and Related Phenomena, Edited by Gordon & Breach Science Publishers, Inc., New York, 1967, 407 pp.

[11] M.J. Bannister, J. Am. Ceram. Soc. 51(10) (1968) 548.
[12] J.L. Woolfrey, M.J. Bannister, J. Am. Ceram. Soc. 55(8) (1972) 390.
[13] R-R. Lee, A.H. Heuer, J. Am. Ceram. Soc. 12(3) (1991) 12.
[14] C.J. Howard, R.J. Hill, J. Mater. Sci. 26 (1991) 127.
[15] J.F. Shackelford, Introduction to Materials Science for Engineers, MacMillan Publ., New York, 1985.
[16] A. Ikesue, S-I. Matsuda, S-J. Shirasaki, Taikabutsu Overseas 12(3) (1991) 12.
[17] H.U. Anderson, J. Am. Ceram. Soc. 50(5) (1967) 235.
[18] P.J. Jorgensen, 407 pp. in Ref. 10.
[19] A. Dietzel, H. Tober, Ceram. Abstr. January (1954) 23a.
[20] L.W. Coughanour, R.S. Roth, S. Marzullo, F.E. Sennet, J. Research Natl. Bur. Standards 54(4) (1955) 191–99; RP 2580.
[21] N. Claussen, R. Wagner, L.J. Gauckler, G. Petzow, J. Am. Ceram. Soc. 61(7–8) (1978) 169.
[22] N. Claussen, J. Jahn, J. Am. Ceram. Soc. 61(1–2) (1978) 94.
[23] R.S Nasar, Dr. Thesis, UFSCar, Jun. (1994) 44 pp., São Carlos - SP, Brazil.